

钢坯闪光焊接系统虚拟试验

卢 宁

(北京建筑大学 机电与车辆工程学院, 北京 100044)

摘 要: 根据钢材无头轧制系统中大截面钢坯闪光焊接的特点, 分别在动力学仿真软件 ADAMS 中建立焊接设备的机械运动学模型, 在 AMESim 中建立闪光焊接顶锻液压伺服系统的非线性模型, 并在 MATLAB 软件工具包 Simulink 中建立焊接系统的伺服控制系统的模型, 通过分析仿真软件两两之间的数据传输接口特性, 建立以 MATLAB 软件为载体的数据动态共享通道, 在 Simulink 中分别调用并启动 AMESim 软件中的液压系统模型和 ADAMS 软件中的机械系统模型, 建立了焊接机电液一体化系统的完全数字平台, 实现了大截面钢坯闪光焊接系统的机电液一体化虚拟试验研究。

关键词: 钢坯; 闪光焊; 虚拟试验

中图分类号: TG 456.9 文献标识码: A 文章编号: 0253-360X(2014)05-0083-05

0 序 言

论文中提出一种新的闪光焊接虚拟试验方法, 分别在 ADAMS 软件中建立对象的机械运动学模型, 在 AMESim 中建立液压系统的非线性模型和在 Simulink 中建立系统的控制系统模型, 通过分析软件之间的接口特性, 建立完善的数据动态共享通道, 实现机电液一体化系统的完全数字平台, 并对闪光神经元复合控制方法^[1]和顶锻过程^[2]预测控制方法进行试验分析和虚拟试验。

1 虚拟试验平台的搭建

1.1 虚拟试验基本理论

钢坯闪光焊接液压系统虚拟试验系统包括闪光焊机机械系统、焊机液压系统和焊接控制系统。如图 1 所示为焊接系统试验平台, 其中机械系统由动力学仿真软件 ADAMS 实现, 液压系统由 AMESim 软件实现, 控制系统则在 Simulink 中设计。虚拟试验是在 3 个仿真软件中分别建立不同部分的模型, 然后通过它们之间的接口进行数据传输, 实现焊接系统的机电液一体化联合虚拟试验。

图 2 为焊接液压系统虚拟试验数据传输原理。其中, 控制系统的输出控制信号为液压系统液压阀的控制信号, 液压系统执行元件(液压缸)驱动焊机机械系统相应元件动作, 机构运动产生的位移信号

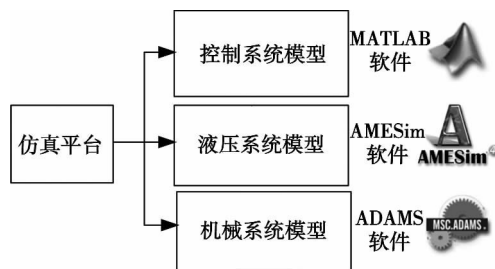


图 1 焊接系统试验平台

Fig. 1 Test platform of welding system

反传给控制系统。根据以上原理建立了相应的虚拟试验平台数据传输图(图 3)。

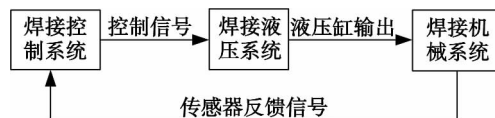


图 2 焊接液压系统虚拟试验数据传输原理图

Fig. 2 Welding principle diagram of the hydraulic system of virtual experiment data transmission

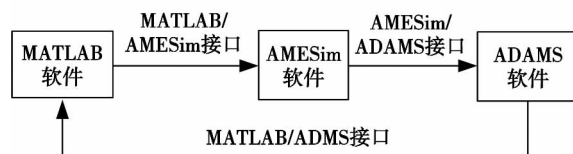


图 3 软件间虚拟试验平台数据传输图

Fig. 3 Virtual test platform for data transmission between software diagram

由图 3 可以看出,不同软件之间的数据是否能够成功传输,完全依靠他们之间的接口是否有效。目前基于 ADAMS 软件的机械系统与基于 MATLAB 的控制系统之间的接口已经成熟; AMESim 软件与 MATLAB 软件的接口也已经成熟; ADAMS 软件与 AMESim 软件的接口也已推出,因此 3 个软件之间进行两两联合仿真没有障碍;然而 3 个软件之间进行联合仿真,国内仍没有成功案例。

文中提出了另外一种联合仿真的方案(图 4),实现了基于 ADAMS、MATLAB 和 AMESim 3 个软件的机械系统、控制系统和液压系统的联合虚拟仿真。图 4 中 AMESim 软件与 ADAMS 软件之间的数据交换以 MATLAB 为平台,液压系统的输出首先通过 AMESim 与 MATLAB 的接口传输到 MATLAB 中,然后通过 ADAMS 软件与 MATLAB 的接口传输给机械系统虚拟样机。

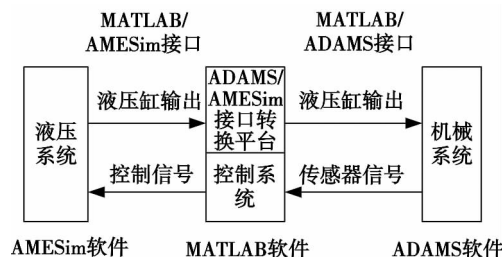


图 4 联合仿真方案

Fig. 4 Combined simulation scheme

1.2 AMESim 软件与 ADAMS 软件变量传输平台的实现

虚拟样机中执行动作的机械系统模型和工作动力的提供者液压系统模型有着密切的关系。机械系统承受液压系统输出的液压力和外界负载的共同作用,遵循机械动力学运动定理和机构模型的约束条件产生机构运动,输出表现各种运动特性的参数,如(角)速度、(角)位移等,如图 5 所示。

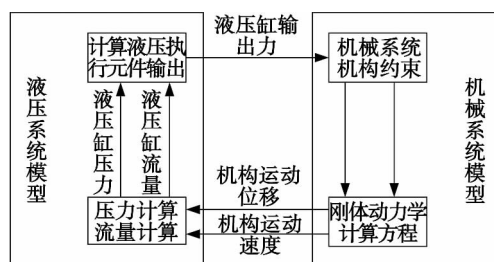


图 5 AMESim 与 ADAMS 仿真接口数据传输平台

Fig. 5 AMESim and ADAMS simulation interface data transmission platform

液压缸输出力是液压缸作用面积和压力的函数,即

$$F_y = Ap \quad (1)$$

机构直线运动方程为

$$\dot{s} = \frac{1}{m} \cdot \int \sum F dt \quad (2)$$

$$s = \int \dot{s} dt + s_0 \quad (3)$$

式中: F 为液压力 F_y 与负载力之和; m 为机构系统的质量; s 为机构位移; \dot{s} 为机构运动速度; A 为活塞面积; p 为液压油压力; t 为作用时间; s_0 为初始位移。

反过来机械系统参数也影响着负载和液压系统的作用情况。机械系统模型对负载的影响主要是工作状态的变化引起负载大小的变化,从而引起机构运动速度和位移的变化,这些参数对液压系统模型状态的影响主要集中在液压系统流量和液压缸压力区体积上。

活塞杆运动的流量方程为

$$Q = A \cdot \dot{s} \quad (4)$$

液压缸内进油腔内液压油体积为

$$V = A \cdot s \quad (5)$$

此液压缸压力区体积是活塞杆位移的函数,流量是活塞杆速度的函数;因此焊机机械系统模型中的 s 、 \dot{s} 状态值直接影响液压系统模型中压力区的液压油体积和系统流量的变化。液压缸外部变量见图 6。

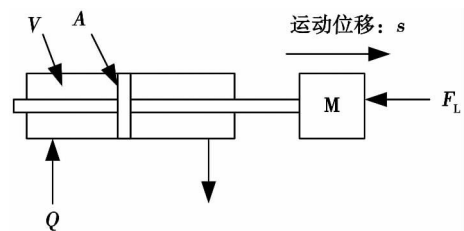


图 6 液压缸外部变量图

Fig. 6 Hydraulic cylinder figure for external variables

虚拟样机环境中将机械系统和液压系统集成就是将上述所有相关的状态参数相互传递、引用,产生类似实际焊机中两个系统间的有机关联:机械系统模型中的驱动力的大小引用液压系统模型中的液压力的输出,同时在液压系统模型各元件的压力和流量方程中直接引用机械模型中各个关键点的速度、位移函数。

根据以上分析,ADAMS 与 AMESim 的接口可以采用以下形式,见图 7。

图 7 中将 AMESim 软件中的液压系统模型液压

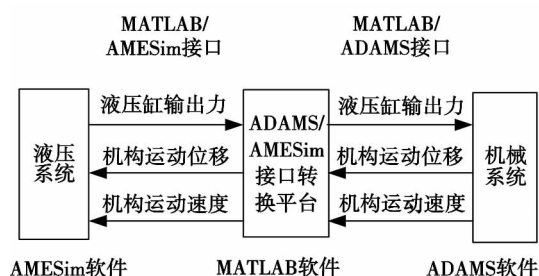


图7 ADAMS与AMESim接口方案

Fig. 7 ADAMS with AMESim interface scheme

缸的输出力信号经过 MATLAB 软件传递给 ADAMS 软件的机械系统模型; 同时 ADAMS 软件的机械系统模型的运动速度和位移信号经过 MATLAB 软件传递给 AMESim 软件中的液压系统模型的液压缸. 这样借助于 MATLAB 就可以实现 ADAMS 与 AMESim 的接口.

2 闪光焊接系统试验

钢坯的闪光焊接属于大截面连续闪光对焊, 焊

接工艺主要由闪光阶段和顶锻阶段两个阶段组成^[3], 闪光阶段负载力比较小, 焊接 200 mm × 200 mm 截面的方形钢坯时, 闪光余量约 20 mm; 顶锻阶段要求夹具能够瞬间提供较大的顶锻速度和顶锻力, 顶锻时间一般小于 1 s, 顶锻力要达到 1 600 kN 以上, 顶锻余量约 30 mm^[1]. 图 8 为在 ADAMS 软件中建立的闪光焊机结构虚拟样机^[4-6], 图 9 为 AMESim 软件中建立的闪光焊机液压系统虚拟模型^[7-8].

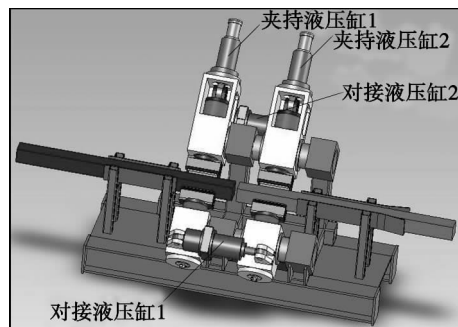


图8 机械系统虚拟样机

Fig. 8 Mechanical system virtual prototyping

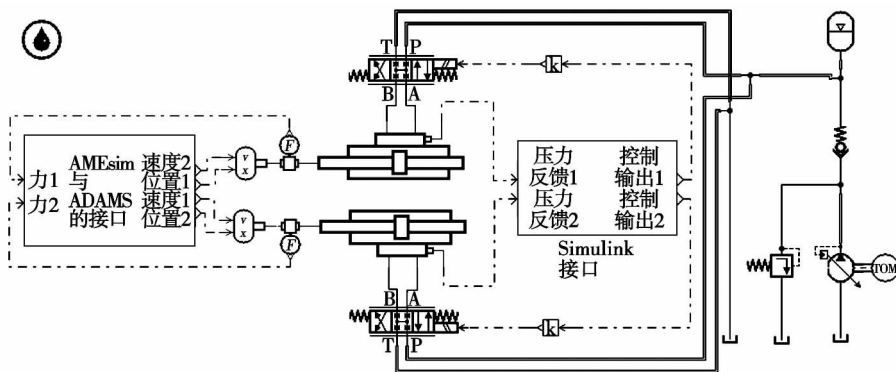


图9 闪光焊机液压系统

Fig. 9 Flash welding machine hydraulic system

图 10 为闪光焊机控制系统在 Simulink 中的实现, 位置输入信号为加速度输入信号 $r_1 = 0.005 t^2 \text{ m}$, 位置控制器为闪光焊接闪光阶段的神经元控制器; 压力输入信号为阶跃信号 $r_2 = 2.0 \times 10^7 \text{ Pa}$, 压力控制器为顶锻阶段压力反馈控制器与误差预测同步控制器的实现; 转换开关 1、2 用来在闪光阶段位置控制与闪光阶段压力控制之间进行切换, 它们之间的转换由总体控制时间(定时时钟)控制, 仿真周期 25 s, 控制时序如下. (1) 7 ~ 15 s 之间转换器接通闪光控制器与液压系统, 完成闪光过程控制. (2) 15 ~ 17 s 之间转换器接通压力控制器与液压系统, 进行对接过程控制. (3) 17 ~ 18 s 取消顶锻力.

进行虚拟试验时, 同时考虑了夹持液压系统的动作时间, 时序如下. (1) 3 ~ 4 s 开始夹持动作; (2) 5 ~ 5.5 s 增压缸开始增压; (3) 18 ~ 18.5 s 增压缸减压; (4) 19 ~ 20 s 夹钳开始返回.

3 虚拟试验结果

3.1 液压缸输出力

液压缸输出力如图 11 所示, 由图 11 可知系统顶锻时的输出力达到 160 t, 满足系统顶锻力的设计要求.

3.2 液压缸输出位移曲线

液压缸输出位移曲线见图 12. 由图 12 可知, 闪

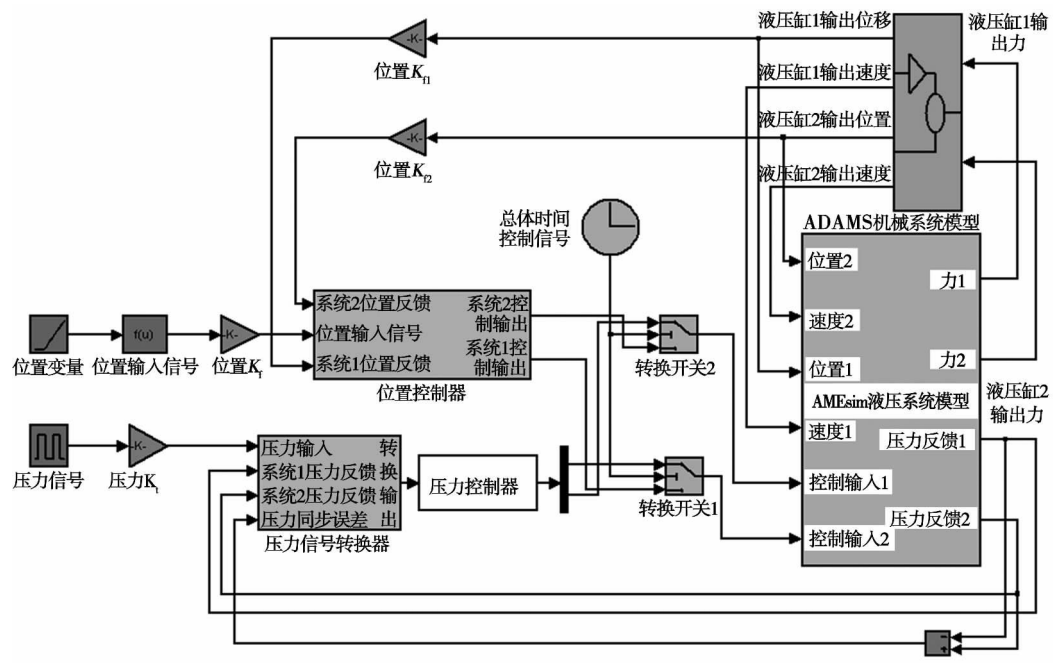


图 10 闪光焊机控制系统

Fig. 10 Flash welding machine control system

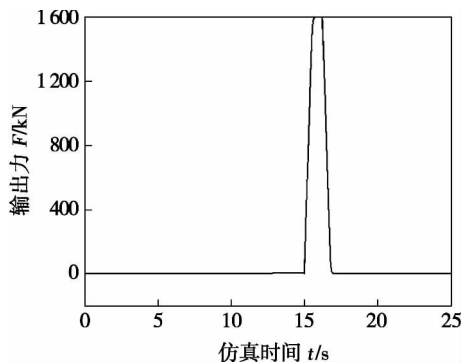


图 11 闪光焊系统输出力曲线

Fig. 11 Flash welding system output force curve

光焊闪光阶段液压缸输出位移约 32 mm, 满足闪光流量(大于 30 mm)的要求; 顶锻阶段位移约 30 mm

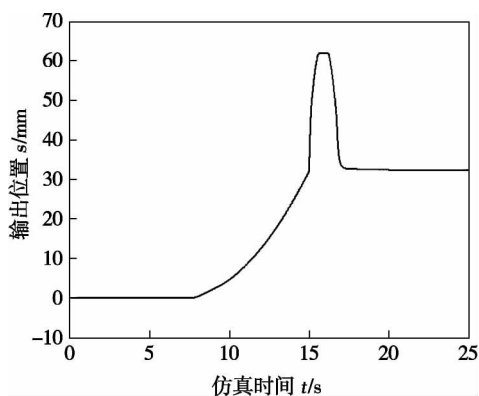


图 12 闪光焊系统输出位移曲线

Fig. 12 Flash welding system output displacement curve

满足顶锻余量(30 mm)的要求。

3.3 负载速度

闪光焊系统输出速度曲线见图 13。由图 13 可知系统顶锻时的输出速度 $v > 100 \text{ mm/s}$, 满足系统 $v > 30 \text{ mm/s}$ 的设计要求。

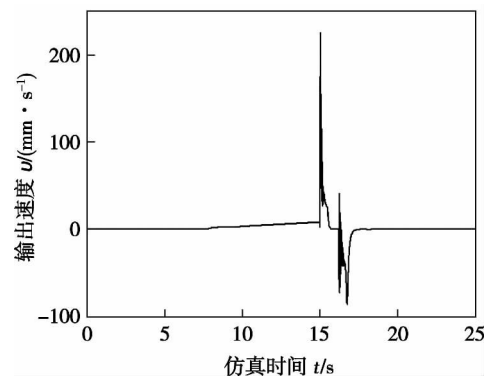


图 13 闪光焊系统输出速度曲线

Fig. 13 Flash welding system output speed curve

4 结 论

(1) 分别在软件 ADAMS, AMESim 和 Simulink 中建立了钢坯闪光焊机机械系统模型、液压系统模型和混合控制系统模型, 并根据软件之间接口特性建立了基于 MATLAB 平台的液压系统和机械系统的接口, 实现了钢坯闪光焊机电液一体化联合虚拟试验。

(2) 利用虚拟试验平台对文中提出的控制方法进行验证。结果表明,虚拟试验平台能够满足要求,设计的控制器满足钢坯闪光焊接液压系统的设计要求。

参考文献:

- [1] 卢宁,付永领,孙新学. 单神经元在液压系统中的应用与电液联合仿真[J]. 系统仿真学报, 2006, 18(11): 3180-3186.
Lu Ning, Fu Yongling, Sun Xinxue. Application of single neuro controller in hydraulic servo system and Co-simulation of electro-hydraulic system [J]. Journal of System Simulation, 2006, 18(11): 3180-3186.
- [2] 卢宁,付永领,孙新学. 预测控制在钢坯闪光焊顶锻控制系统中的应用[J]. 焊接学报. 2006, 27(9): 85-88.
Lu Ning, Fu Yongling, Sun Xinxue. Pre-controller is used in press synchronism control system of bill flash butt welding [J]. Transactions of the China Welding Institution, 2006, 27(9): 85-88.
- [3] 朱正行,严向明,王敏. 电阻焊技术[M]. 北京:机械工业出版社, 2000.
- [4] Poirier. 晶体的高温塑性变形[M]. 关德林,译. 大连:大连理工大学出版社, 1989.
- [5] 孙新学,付永领,卢宁. 闪光焊机的移动控制策略与仿真分析[J]. 焊接学报, 2008, 29(9): 15-18.
Sun Xinxue, Fu Yongling, Lu Ning. Travelling control for flying type flash-butt welder and its simulating analysis [J]. Transactions of the China Welding Institution, 2008, 29(9): 15-18.
- [6] 王治平,王克争. 500 kW 预热闪光焊工艺试验[J]. 焊接学报, 2000, 21(4): 76-79.
Wang Zhiping, wang Kezheng. Technological experiment of 500 kW preheating flash butt welding [J]. Transactions of the China Welding Institution, 2000, 21(4): 76-79.
- [7] 宋义学. 袖珍液压气动手册[M]. 北京:机械工业出版社, 1995.
- [8] 卢宁,付永领,孙新学. 钢坯闪光焊接液压系统研究[J]. 液压与气动, 2005(7): 3-6.
Lu Ning, Fu Yongling, Sun Xinxue. Development of hydraulic system for steel bill flash butt welding [J]. Chinese Hydraulics & Pneumatics, 2005(7): 3-6.

作者简介: 卢宁,男,1976年出生,博士,高级工程师. 主要从事液压系统、城市轨道交通、机电控制方面的工作. 发表论文20余篇. Email: luning@bucea.edu.cn

书讯

宋天虎副理事长、潘际銮院士及德国莱布尼兹大学 D. Rehfeldt 教授倾情作序



书号: 978-7-111-37325-4
定价: 49.00元

《焊接电弧现象与焊接材料工艺性》

王宝 宋永伦 著 林尚扬 审

本书以对焊接电弧现象的大量、细致的观察为切入点,揭示熔滴过渡现象与工艺性之间的具体联系。

通过焊接质量分析仪提取反映某些工艺状态的电弧现象的数据信息,用电弧物理指数加以描述,从该类电弧过程的属性寻求有效的分析方法,提出了对其特征现象及物理意义的定量认识和解读。

将对焊接材料工艺性的评价由人的直感和经验提升到信息化、知识化的层面上,从而实现焊接材料分析与评价的定量化。

编辑热线: 010-88379733 购书热线: 010-88379425 传真: 010-68351729 网络购书支持: 中国科技金书网

传真购书请注明: 姓名、详细地址、邮编、联系电话、传真、E-mail、所购图书书名、书号、数量、是否需要发票及发票抬头

sing this technique , experiments were conducted in 4 mm thick sheets of aluminum alloy 5A02 in H14 condition. The results show that the bonding widths of cross-FSSW joints had been increased , the adverse effects of interface distortion and the lack of material of the keyhole had been avoided. cross-FSSW joints were found to be superior to traditional Friction stir spot welds produced under optimum conditions in lap-shear.

Key words: cross-friction stir spot welding; friction stir welding; aluminum alloy; mechanical properties

The theory and application of the virtual fatigue test of welded structures based on the master S – N curve method

ZHAO Wenzhong¹ , WEI Hongliang^{1,2} , FANG Ji¹ , LI Jitao¹ (1. School of Traffic and Transportation Engineering , Dalian Jiaotong University , Dalian 116028 , China; 2. Technical Center of Qiqihar Rail Traffic Equipment Co , Qiqihar 161002 , China) . pp 75 – 78

Abstract: The necessity and feasibility of the virtual fatigue test technology of welded structure were discussed firstly. Then a basic theory of a new method called the master S – N curve method , which can be used for assessment of fatigue life of welded structure and published by the ASME (2007) standard , has been discussed as well. Following this discussion , a conclusion has been given that is the new method is resulted from the welded structure fatigue failure mechanism instead of fatigue failure test data. So this method is more suitable as the core algorithm in welding virtual fatigue test than nominal stress method. Finally , two applications have been given , and the results show that during the design phase , the welded structure virtual fatigue test technology based on the master S – N curve method , can effectively identify stress concentrations happened at each weld in a complex welding structure. In fact , this just is needed in design process.

Key words: welded structure; fatigue damage; virtual fatigue test; the master S – N curve; stress concentration

Laser welding technology of multi-chip subsystem shell and cover

YU Shenglin^{1,2} , XUE Songbai¹ , YAN Wei³ , JI Xu-an² , ZHU Xiaojun³ (1. College of Materials Science and Technology , Nanjing University of Aeronautics and Astronautics , Nanjing 210016 , China; 2. Nanjing University of Information Science and Technology , Nanjing 210044 , China; 3. Nanjing Research Institute of Electronics Technology , Nanjing 210039 , China) . pp 79 – 82

Abstract: Adopted the advantages of laser welding and by use of ANSYS software , the structure of the Al-50Si shell and the cover (4047 aluminum alloy) of the multi-chip subsystems which sealed by laser welding was analyzed , and the physical verification was also carried out. It was proved that structure form is the key factor which affected the quality of multi-chip subsystems which sealed by laser welding , the stress in laser weld of square structure is 36% higher than that in special-shaped structure (according to ANSYS analysis results) , and the air tightness of the square structure is lower by almost one order of magnitude than that of special-shaped structure , which performed by physical verification. The reason is that after laser welding , the welding

cracks induced by welding stress in the weld of square structure , so as to affect the air tightness of the weld. By adopt of special-shaped structure of multi-chip subsystems made from Al-50Si composite materials and the cover made from 4047 aluminum alloy , the stress in the welds can be effectively reduced , so the cracks in the weld are actually avoidable during laser welding. The result was indicated that the helium leak rate of the weld of special-shaped structure can reach to $8.9 \times 10^{-9} \text{ Pa} \cdot \text{m}^3/\text{s}$, which met the hermetic package requirement of multi-chip subsystems.

Key words: multi-chip; Al-Si alloys; laser welding; leakage rate

Virtual weld experiment system of billet flash butt welding process

LU Ning (School of Mechanical-Electronic and Automobile Engineering , Beijing University of Civil Engineering and Architecture , Beijing 100044 , China) . pp 83 – 87

Abstract: In view of the characteristics of flash welding system for large section rolling steel billet , mechanical kinematic models of welding equipments were built by using dynamics simulation software ADAMS. In which forging hydraulic servo system nonlinear model of the flash butt welding process was proposed in AMESim. Moreover , the servo control system for virtual welding system was built by utilizing the Simulink package of MATLAB software. By analysis of the data transmission characteristics between simulation softwares , a shared channel for dynamic data carrier was established by MATLAB software. A digital platform of welding electromechanical system was brought into forward , by which virtual experiment on electromechanical system of billet flash welding process can be carried out.

Key words: billet; flash butt weld; virtual experiment

Analysis of principle of least action on explosive welding process

SHI Changgen , ZHAO Linsheng , HOU Hongbao , WANG Yu (PLA University of Science Technology , Nanjing 210007 , China) . pp 88 – 90

Abstract: The principle of least action , basic law of the nature and the final rule of the physics , was found to be followed by the explosive welding process by theoretical analysis and interface test. Namely the optimal welding interface can be obtained with the least explosive charge. The bonding energy of the interface can be looked upon the action on the course. To minimize the bonding energy , these rules must be followed such as the lower limit of explosive charge , the upper limit of span and the explosive of the lower critical explosion velocity. The principle of least action is achieved on the explosive welding process , and the bonding interface will be best.

Key words: explosive welding; bonding interface; upper limit; lower limit

Investigation of thermal shock resistance of the nanostructured zirconia thermal barrier coatings treated by laser glazing

WANG Hongying , LI Zhijun , TANG Weijie , HAO Yunfei (Shenzhen Polytechnic , Shenzhen 518055 , China) . pp 91 – 94

Abstract: The nanostructured zirconia coatings were pre-